Journal of Solid State Chemistry **152,** 577–581 (2000)
doi:10.1006/jssc.2000.8752, available online at http://www.idealibrary.com on IDEAL®

RAPID COMMUNICATION

Magnetic Order in Perovskite $Pr_{1-x}Ba_xCoO_3$ Studied by Magnetic Circular Dichroism (MCD) Spectroscopy

K. Yoshii,* M. Mizumaki,† Y. Saitoh, and A. Nakamura‡

*Japan Atomic Energy Research Institute (JAERI), Mikazuki, Hyogo 679-5148, Japan; †Japan Synchrotron Radiation Research Institute (JASRI), Mikazuki, Hyogo 679-5198, Japan; and ‡Japan Atomic Energy Research Institute (JAERI), Tokai, Ibaraki 319-1195, Japan

Received February 10, 2000; in revised form April 3, 2000; accepted April 20, 2000

Magnetic properties have been studied for the perovskite $Pr_{1-x}Ba_xCoO_3$ ($0 \le x \le 0.5$). Ferromagnetic order is observed below $\sim$190 K for $x \ge 0.2$ in dc susceptibility–temperature curves. Magnetic circular dichroism spectra were measured for a ferromagnetic phase at Co–$L_{2,3}$, Pr–$M_{4,5}$, Ba–$M_{4,5}$, and O–K edges. It is revealed that the Co ion has both spin and orbital moments. It is also observed that the Ba 4*f* orbitals have a localized moment and exhibit ferromagnetic order at low temperatures, though Ba^{2+} is expected to be almost only in a nonmagnetic $4f^0$ state. Magnetic order is observed also for Pr 4*f* and O 2*p*. © 2000 Academic Press

Recently, much attention has been received on perovskite cobaltates $Ln_{1-x}A_xCoO_3$ (Ln = lanthanides, A = alkaline earth metals) because of their interesting and unusual physical properties (1–10). The end compounds $LnCoO_3$ containing Co^{3+} are semiconductors or insulators with no magnetic order. Doping of the A-ions ($Ln_{1-x}A_xCoO_3$) introduces the oxidized ion Co^{4+}, leading to the ferromagnetic order with Curie temperatures (T_C) below $\sim$250 K. $La_{1-x}A_xCoO_3$ with A = Sr and Ba are metallic ferromagnets. The compounds containing heavier lanthanides exhibit semiconductive or insulating behavior. Magnetic properties have been most extensively studied for $La_{1-x}Sr_xCoO_3$ ($0 \le x \le 0.5$) (1–4), where the very complex behaviors are observed against x, and have been discussed in detail (1). There exist the three spin states of Co^{3+} and Co^{4+}, i.e., LS (low-spin), IS (intermediate-spin), and HS (high-spin) states. This system with $x < 0.1$ shows superparamagnetic or spin-glass behavior due to a formation of hole-rich clusters where low-spin (LS) Co^{4+} ($t_{2g}^5 e_g^0$) and intermediate-spin (IS) Co^{3+} ($t_{2g}^5 e_g^1$) are ferromagnetically coupled. For $0.1 \le x \le 0.18$, the size of each IS cluster becomes larger. As the magnetic interactions between the clusters are antiferromagnetic, spin-glass behavior is observed. In the larger x region, the cluster becomes large enough to change the system into metallic ferromagnets accompanied by cluster-glass phenomena.

For other systems, there have been comparably few reports on their properties so far except those such as for $Ln_{0.5}Ba_{0.5}CoO_3$ (Ln = lanthanides) (6,7), $Gd_{1-x}Sr_xCoO_3$ (8), and $Pr_{1-x}Sr_xCoO_3$ (9,10). In this paper, magnetic properties of $Pr_{1-x}Ba_xCoO_3$ ($0 \le x \le 0.5$) were studied by dc magnetization measurements. Magnetic circular dichroism (MCD) spectroscopy (11) was adopted to obtain the information of spin and orbital moments in a ferromagnetic phase.

The $Pr_{1-x}Ba_xCoO_3$ (x = 0, 0.1, 0.2, 0.3, 0.4, 0.45, and 0.5) samples were prepared by the ceramic method. Stoichiometric mixtures of Pr_2O_3 (3N, Soekawa), $BaCO_3$ (4N, Soekawa), and CoO (3N, High Purity Chem. Lab.) were fired in air at 1200°C for 24–48 h. The firing was repeated two to three times. The oxygen contents were determined from thermogravimetry in a reducing atmosphere. The δ values for $Pr_{1-x}Ba_xCoO_{3-\delta}$ are 0–0.03 for $x \le 0.1$, 0.05–0.08 for x = 0.2–0.3, 0.07–0.11 for x = 0.4, and 0.10–0.12 for $x \ge 0.45$ ($\pm$0.02). The increase in δ with x is the same trend as that for $Pr_{1-x}Sr_xCoO_3$ (9) and $Gd_{1-x}Sr_xCoO_3$ (8). The value for x = 0.5 is close to that of $Tb_{0.5}Ba_{0.5}CoO_3$, δ = 0.13 (7). Roughly, the contents of Co^{4+} around x = 0.5 are estimated to be $\sim$50–60% of those for the oxygen stoichiometric samples. For convenience, the samples will be denoted as $Pr_{1-x}Ba_xCoO_3$ in most of the discussion. Powder X-ray diffraction (XRD) measurements (MAC Science Co., M03XHF^{22}) revealed that their crystal structures are the orthorhombic perovskite type (*Pnma*; $GdFeO_3$ type). dc magnetization measurements were carried out with a SQUID magnetometer (Quantum Design MPMS). Other details have been given elsewhere (10).

The MCD spectra were measured for the x = 0, 0.1, and 0.4 systems using synchrotron radiation at a soft X-ray

0022-4596/00 $35.00

beamline BL25SU of SPring-8, Japan (12). Sample surfaces were thoroughly filed in an analysis chamber before the measurements. The spectra were obtained from the subtraction of XANES (X-ray absorption near edge structure) spectra, which were measured at $\sim$40 K in a total electron yield mode around Co–$L_{2,3}$, Pr–$M_{4,5}$, Ba–$M_{4,5}$, and O–K edges. A magnetic field of $\pm$1.4 T was applied to the samples and was switched at each photon energy to flip the magnetization.

Figure 1 shows dc susceptibility–temperature (χ–T) curves between 4.5 and 300 K with an applied field (H) of 100 Oe. The curve of $PrCoO_3$ was confirmed to resemble that previously reported (13). This compound exhibits no magnetic order, since the Co^{3+} ions are in a nonmagnetic LS state ($L = S = 0$) below 300 K (13). With substituting Ba for Pr, the Co ions are partially oxidized to Co^{4+}, leading to the obvious ferromagnetic transitions with Curie temperatures (T_C) of $\sim$150–190 K for $x \geq 0.2$.

For the curve of $x = 0.1$, inflection is observed around 40 K. As a Weiss temperature was found to be close to zero, this might be owing to a spin-glass transition brought about by the competition between ferromagnetic and antiferromagnetic interactions. Indeed, the compound showed both logarithmic time dependence of magnetization at 4.5 K and a susceptibility cusp only for the ZFC (zero-field-cooled) curve, indicating the existence of spin- or cluster-glasses as in $La_{1-x}Sr_xCoO_3$ (1–4). However, the aging effect, characteristic of spin-glasses (4), has not been observed so far. These phenomena have been found also for $x \geq 0.2$.

The curve of $Pr_{0.5}Ba_{0.5}CoO_3$ with $T_C \sim 150$ K has a similar profile to that in the previous work (7). T_C has a maximum ($\sim$190 K) around the composition $x = 0.3$–0.4. This

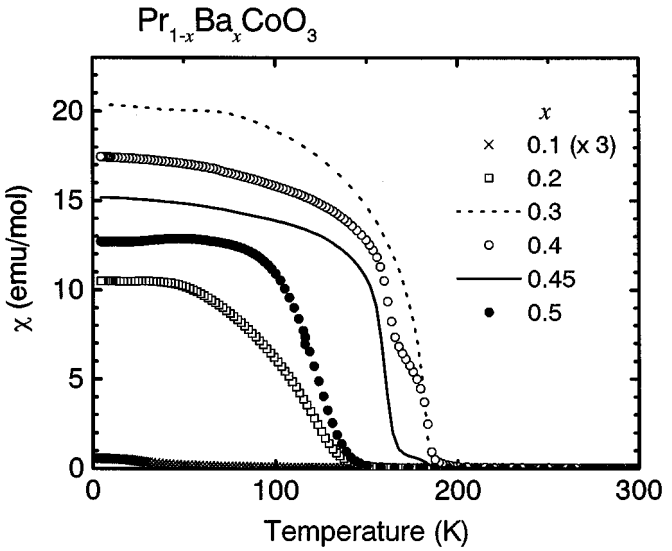

FIG. 1. χ–T curves for all the $Pr_{1-x}Ba_xCoO_3$ systems in FC (field-cooled) condition with an applied field of $H = 100$ Oe. Susceptibilities for $x = 0.1$ are multiplied by a factor of 3.

is different from the behavior of the $Ln_{1-x}Sr_xCoO_3$ systems where T_C tends to monotonically increase as x is increased (1, 2, 4, 5, 9). Two of the authors have investigated also the magnetic properties of $Pr_{1-x}Sr_xCoO_3$ and found the monotonic increase in T_C up to $\sim$250 K with increasing x (10). As is well known, the value of T_C strongly depends on both a Co–O–Co angle and a Co–O length. From the Rietveld analyses for the XRD data using RIETAN (14), a Co–O–Co shows a maximum for $Pr_{1-x}Ba_xCoO_3$ ($\sim 175^\circ$ at $x = 0.4$) (15), while a Co–O length tends to decrease with increasing x. Thus the present behavior is understood in terms of the enhancement of exchange interactions due to the increase in the Co–O–Co angle. On the other hand, for $Pr_{1-x}Sr_xCoO_3$, the angle tends to increase with increasing x (15).

For $0.4 \leq x \leq 0.5$, the values of T_C in this system are lower than those for $La_{1-x}Sr_xCoO_3$ and $Pr_{1-x}Sr_xCoO_3$ in the same x region ($\geq \sim$ 220–230 K) obtained in this work and Ref. (10), where T_C becomes higher with increasing x. It was verified that each T_C was close to those reported in Refs. (1, 2, 4, and 9). From the Rietveld analyses, no obvious relationship between the crystal structures and T_C was obtained in these three systems. A possible origin is the slightly larger oxygen deficiencies δ in $Pr_{1-x}Ba_xCoO_{3-\delta}$ than those for $La_{1-x}Sr_xCoO_{3-\delta}$ and $Pr_{1-x}Sr_xCoO_{3-\delta}$ where δ is less than $\sim$0.06 (2,9). Similar values were obtained for these systems also in the present work. For $La_{1-x}Sr_xCoO_3$ with $x > 0$, the doping of Sr introduces the LS Co^{4+} ion, which stabilizes the IS Co^{3+} (1). Thus the dominant spin states are the LS Co^{4+} and the IS Co^{3+}. Assuming the same situation for the other systems, the content of the IS Co^{3+} ions might be lower in $Pr_{1-x}Ba_xCoO_3$ due to the lower content of Co^{4+}. The other Co^{3+} ions are considered to remain in the nonmagnetic LS Co^{3+}, whose population is larger than in $La_{1-x}Sr_xCoO_3$ and $Pr_{1-x}Sr_xCoO_3$. This leads to weaker magnetic interactions and smaller localized moment per unit formula. As is shown below, the ordered magnetic moment determined from MCD is smaller than that of $La_{1-x}Sr_xCoO_3$. This is qualitatively consistent with this speculation, though the magnetic structure is to be determined for quantitative discussion. The maximum of T_C at $x = 0.3$–0.4 might be explained also in this context, considering that the oxygen deficiency becomes larger with increasing x.

Figure 2 shows the XANES spectra around the Co–$L_{2,3}$ and Ba–$M_{4,5}$ edges for $PrCoO_3$, $Pr_{0.9}Ba_{0.1}CoO_3$, and $Pr_{0.6}Ba_{0.4}CoO_3$. They are normalized by the intensities of the Co–L_3 absorption peaks. Based on the dipole selection rule, the Co–$L_{2,3}$ ($2p_{1/2,3/2}$) and Ba–$M_{4,5}$ ($3d_{3/2,5/2}$) peaks correspond to the absorption to Co–$M_{4,5}$ ($3d_{3/2,5/2}$) and Ba–$N_{6,7}$ ($4f_{5/2,7/2}$) shells, respectively. Since the spectral profile of $PrCoO_3$ is close to that of $LaCoO_3$ at 300 K (16), the Co^{3+} ions are mainly in the LS state. This result is consistent with the magnetic data in Fig. 1 and the discussion in Ref. (13). The sharp Ba–$M_{4,5}$ absorption peaks

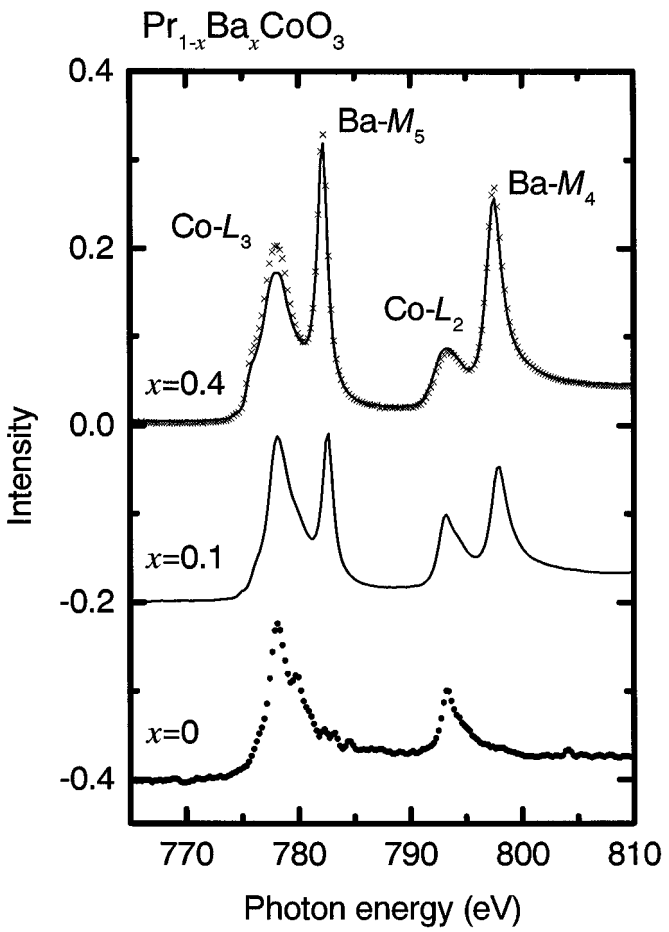

FIG. 2. XANES spectra for $Pr_{1-x}Ba_xCoO_3$ with $x = 0, 0.1$, and 0.4 around Co–$L_{2,3}$ and Ba–$M_{4,5}$ edges. The spectra for $x = 0$ and 0.1 were measured with no magnetic field. Cross markers and solid line for $x = 0.4$ stand for parallel and antiparallel alignment of photon spin and magnetization direction, respectively (11).

reveal narrow band widths of the Ba 4*f* orbitals due to their localized nature. It is also noticed that the low energy shoulder at the Co–L_3 peak evolves with increasing x. As was noted, the main spin-states expected are the LS Co^{4+} ($t_{2g}^5 e_g^0$), and IS Co^{3+} ($t_{2g}^5 e_g^1$). Based on the general trend of X-ray absorption, the electron excitation in the highly oxidized ion Co^{4+} is assumed to be located at the higher photon energy side of each absorption peak. Around the center of the peaks, there might exist the photoabsorption to the LS Co^{3+}, due to the large oxygen deficiency noted earlier. Thus the lower energy shoulders are assigned to the photoabsorption to the IS Co^{3+}. The analogous profiles were reported for $LaCoO_3$ at high temperature region above 520 K where the population of the IS or HS ($t_{2g}^4 e_g^2$) state is increased by thermal excitation (16). Based on the theoretical calculations, this shoulder was regarded as the transition to the mixed state of the LS and HS Co^{3+}. Identical spectral profiles found for $La_{1-x}Sr_xCoO_3$ for $x > 0$ (17) imply that the shoulders are rather the transitions to the IS Co^{3+} state in the present system.

Figure 3 shows the MCD spectrum for $Pr_{0.6}Ba_{0.4}CoO_3$, which was obtained from the XANES spectra in Fig. 2. Also the spectrum of $La_{0.6}Sr_{0.4}CoO_{3-\delta}$ ($T_C \sim 240$–250 K, $\delta \sim 0.03$–0.06) is displayed for comparison (17). No obvious MCD effect was observed for both $PrCoO_3$ and $Pr_{0.9}Ba_{0.1}CoO_3$ at ~ 40 K. In the figure, the peaks at the two Co edges indicate the ferromagnetic order of Co 3*d* spin moments (11). The intensity differences between the Co–L_2 and –L_3 MCD effects reveal the existence of a Co 3*d* orbital moment (11). Apparently the LS Co^{4+} ($t_{2g}^5 e_g^0$) and the IS Co^{3+} ($t_{2g}^5 e_g^1$) have both of spin and orbital moments, if the orbital quenching is ignored. The result shows that the 3*d* orbitals are not fully quenched by the crystalline field and is also a direct observation for the origin of the magnetostriction in $La_{1-x}Sr_xCoO_3$ (18).

The profiles of these spectra at the two Co edges are nearly identical. MCD effects at the edges in $Pr_{0.6}Ba_{0.4}CoO_3$ are $\sim 63\%$ of those in $La_{0.6}Sr_{0.4}CoO_3$. It

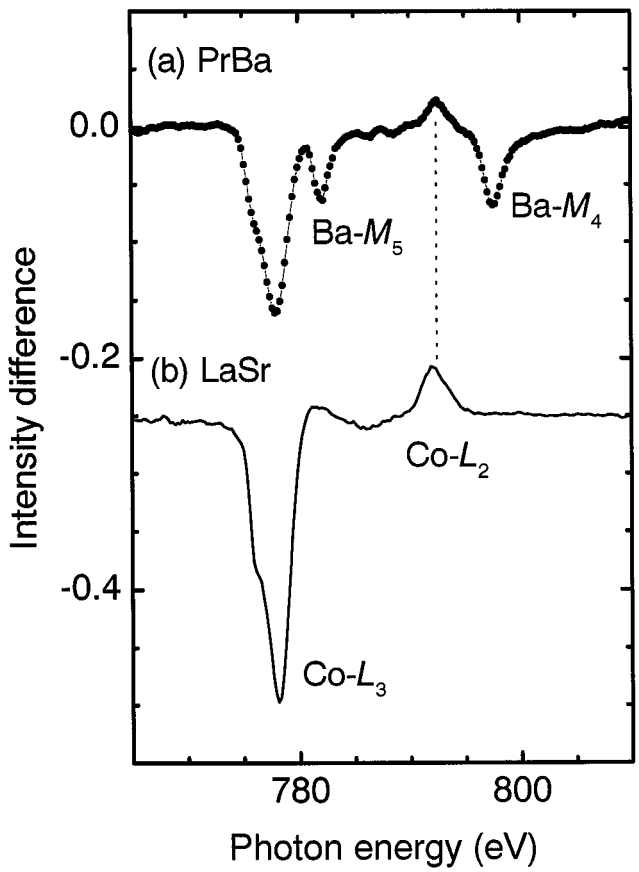

FIG. 3. (a) MCD spectrum for $Pr_{0.6}Ba_{0.4}CoO_3$ (PrBa) obtained from the subtraction of XANES spectra in Fig. 2, (solid line)-(cross markers). Intensity difference is normalized by the intensity of the Co–L_3 absorption peak. (b) The same for $La_{0.6}Sr_{0.4}CoO_3$ (LaSr) (17), where the base line is shifted to around -0.25.

was also found that the XANES spectra of these systems give essentially the same profiles (17). These results mean that the sum rules of MCD (11) lead to $\sim 63\%$ spin and orbital moments compared with those in $La_{0.6}Sr_{0.4}CoO_3$, assuming the same hole number of the Co ions in $Pr_{0.6}Ba_{0.4}CoO_3$ and $La_{0.6}Sr_{0.4}CoO_3$. The spin and orbital moments for $Pr_{0.6}Ba_{0.4}CoO_3$ are $\sim 0.60\ \mu_B$/Co and $\sim 0.21\ \mu_B$/Co, respectively. They are slightly decreased by $\sim 3\%$, if the different hole numbers arising from the oxygen deficiency are taken into account. The smaller moments than in $La_{0.6}Sr_{0.4}CoO_3$ might indicate the larger population of the nonmagnetic LS Co^{3+} ions, as noted earlier.

The figure represents also the two peaks with the MCD effects ($\sim 3\%$) at the Ba–$M_{4,5}$ edges. Although the negative sign of the two MCD peaks cannot be understood only on the basis of the description for MCD usually seen in the reviews (11), the remaining peaks are ascribed to ferromagnetic order of Ba 4*f* moments. An analogous phenomenon was reported for Ce–$M_{4,5}$ edges in a "Kondo-like" semiconductor $CeFe_4P_{12}$, where the MCD effects at both edges have a positive sign (19). This was explained in connection with orbital polarization in Ce 4*f* states. Though this explanation might be applicable also to the present phenomenon, the result is interesting since the Ba ion is considered to be almost only in the ground state Ba^{2+} with no 4*f* electron, $4f^0$. The Ba 4*f* moment originates from the electronic states containing 4*f* electrons, which are generated by either electron excitation in the Ba^{2+} ion, or hybridization of Ba 4f with the atomic orbitals of the other ions, which are generally neglected in qualitative analyses. Theoretical calculations are to be done for understanding both the electronic structure of Ba and the same negative sign of the MCD effects. The direction of the Ba moment is plausibly expected to be the same as that of Co 3*d*, because of an effective magnetic field from Co. An analogous spectrum to that of Ce in $CeFe_4P_{12}$ was obtained also for Pr^{3+} (ground state $4f^2$) at the Pr–$M_{4,5}$ edges, where the MCD effects are smaller than that for Ba, $\sim 1.5\%$.

Figure 4 shows a XANES and an MCD spectra around the O–*K* (1*s*) edge. The O 1*s* electrons are excited to the *np* character orbitals of oxygen hybridized with the La and Co atomic orbitals as indicated in the figure (*n*: principal quantum number) (16). Also the excitation to Ba 5*d*–O *p* orbitals plausibly occurs around the La 5*d*–O *p* excitation region. The profile of the MCD spectrum around the region pointed by an arrow is similar to that of $La_{1-x}Sr_xMnO_3$ (20). As this region consists mainly of the excitation to O 2*p*–Co 3*d* orbitals, the O 2*p* moments have the same direction as the Co 3*d* moments. This result implies the important role of hybridization between Co 3*d* and O 2*p* in the ferromagnetic order.

In summary, magnetic properties were studied for $Pr_{1-x}Ba_xCoO_3$ ($0 \le x \le 0.5$). Ferromagnetic order is observed for $x \ge 0.2$. The MCD spectrum measured at the

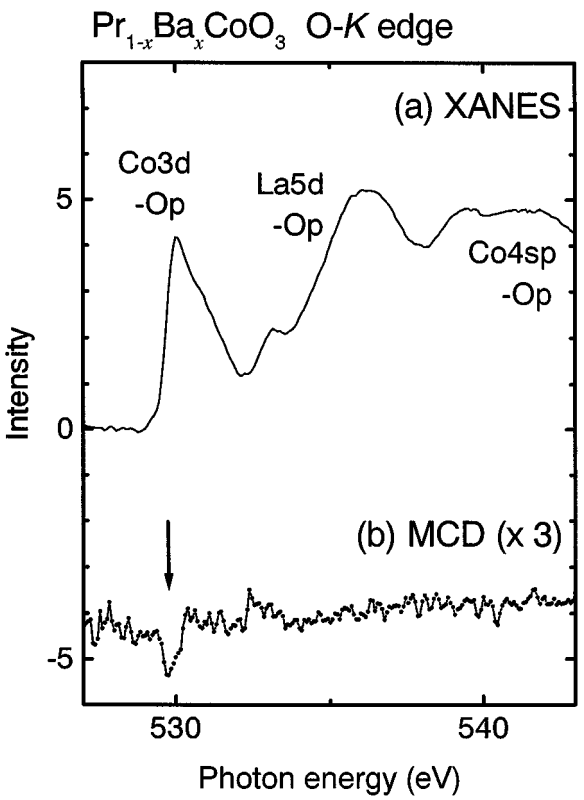

FIG. 4. (a) XANES and (b) MCD spectra for $Pr_{0.6}Ba_{0.4}CoO_3$ around an O–*K* (1*s*) edge. The hybrid orbitals are shown in the XANES spectrum, based on the assignment in Ref. (16). MCD effects are defined as intensity difference and are multiplied by a factor of 3.

Co–$L_{2,3}$ edges indicates that the Co ion has both spin and orbital moments. Ferromagnetic order of the Ba moments is also observed, which reveals the contribution of the electronic states having 4*f* electrons. Magnetic order is found also for Pr 4*f* and O 2*p*.

ACKNOWLEDGMENT

We gratefully thank Dr. M. Kotsugi of Osaka University for his help in the MCD measurements.

REFERENCES

1. R. Caciuffo, D. Rinaldi, G. Barucca, J. Mira, J. Rivas, M. A. Señarís-Rodríguez, P. G. Radaelli, D. Fiorani, and J. B. Goodenough, *Phys. Rev. B* **59,** 1068 (1999). [See references therein]
2. M. A. Señarís-Rodríguez and J. B. Goodenough, *J. Solid State Chem.* **118,** 323 (1995).
3. P. A. Joy and S. K. Date, *J. Phys.: Condens. Matter.* **11,** L217 (1999). [See references therein]
4. M. Itoh, I. Natori, S. Kubota, and K. Motoya, *J. Phys. Soc. Jpn.* **63,** 1486 (1994).
5. C. N. R. Rao, O. M. Parkash, D. Bahadur, P. Ganguly, and S. Nagabhushana, *J. Solid State Chem.* **22,** 353 (1977).

6. Y. Moritomo, M. Takeo, X. J. Liu, T. Akimoto, and A. Nakamura, *Phys. Rev. B* **58,** R13334 (1998).
7. I.O. Troyanchuk, N. V. Kasper, D. D. Khalyavin, H. Szymczak, R. Szymczak, and M. Baran, *Phys. Rev. B* **58,** 2418 (1998).
8. K. H. Ryu, K. S. Roh, S. J. Lee, and C. H. Yo, *J. Solid State Chem.* **105,** 550 (1993).
9. H. W. Brinks, H. Fjellvåg, A. Kjekshus, and B. C. Hauback, *J. Solid State Chem.* **147,** 464 (1999).
10. K. Yoshii and A. Nakamura, *Physica B* (2000), in press.
11. For example, J. Stöhr, *J. Electron Spectrosc. Relat. Phenom.* **75,** 253 (1995).
12. Y. Saitoh, T. Nakatani, T. Matsushita, T. Miyahara, M. Fujisawa, K.Soda, T. Muro, S. Ueda, H. Harada, A. Sekiyama, S. Imada, H. Daimon, and S. Suga, *J. Synchrotron Rad.* **5,** 542 (1998); Y. Saitoh, H. Kimura, Y. Suzuki, T. Nakatani, T. Matsushita, T. Muro, T. Miyahara, M. Fujisawa, K. Soda, S. Ueda, H. Harada, M. Kotsugi, A. Sekiyama, and S. Suga, "Abstract of the 18th International Conference on X-Ray and Inner-shell Processes, Chicago," (1999).
13. M. Itoh, M. Mori, S. Yamaguchi, and Y. Tokura, *Physica B* **259–261,** 902 (1999).
14. F. Izumi, *in* "The Rietveld Method" (R. A. Young, Ed.), Chap. 13, Oxford Univ. Press, Oxford, 1993; Y. -I. Kim and F. Izumi, *J. Ceram. Soc. Jpn.* **102,** 401 (1994).
15. K. Yoshii and A. Nakamura, in preparation.
16. M. Abbate, J. C. Fuggle, A. Fujimori, L. H. Tjeng, C. T. Chen, R. Potze, G. A. Sawatzky, H. Eisaki, and S. Uchida, *Phys. Rev. B* **47,** 16124 (1993).
17. M. Mizumaki *et al.*, in preparation.
18. M. R. Ibarra, R. Mahendiran, C. Marquina, B. García-Landa, and J. Blasco, *Phys. Rev. B* **57,** R3217 (1998).
19. T. Miyahara, H. Ishii, S. Imada, Y. Saitoh, R.-J. Jung, H. Kimura, S. Suga, H. Sugawara, and H. Sato, *Jpn. J. Appl. Phys.* Suppl. **38**(1), 396 (1999).
20. E. Pellegrin, L. H. Tjeng, F. M. F. de Groot, R. Hesper, G. A. Sawatzky, Y. Moritomo, and Y. Tokura, *J. Electron Spectrosc. Relat. Phenom.*, **86,** 115 (1997).